Alternating current plasma operation in the STOR-M tokamak

1996 Nucl. Fusion 36 1335

(http://iopscience.iop.org/0029-5515/36/10/I06)

ALTERNATING CURRENT PLASMA OPERATION IN THE STOR-M TOKAMAK

O. MITARAI[a], Chijin XIAO, Liyan ZHANG[b], D. McCOLL,
Wei ZHANG[c], G. CONWAY[d], A. HIROSE, H.M. SKARSGARD*
Plasma Physics Laboratory,
Department of Physics, University of Saskatchewan,
Saskatoon, Saskatchewan, Canada

ABSTRACT. One cycle alternating current (AC) plasma operation without a dwell time has been achieved in the STOR-M tokamak with good reproducibility using a newly developed ohmic heating circuit. The plasma current of +24 kA is smoothly ramped down in 10 ms with a rampdown rate of around 2.0 kA/ms and then ramped up to between −20 and −24 kA directly without a dwell time. The plasma density of up to $(3.7 \pm 0.6) \times 10^{18}$ m^{-3} remains at the current reversal as observed in recent soft landing experiments. The key to a successful, reproducible and direct transition in AC tokamak operations on STOR-M is to control both the total vertical field by a feedback control system and the plasma density by careful gas puffing during the current reversal phase. This experiment has demonstrated that the initial loop voltage for the second negative current is minimized when the dwell time approaches zero, and the AC operation without dwelling is possible whenever the plasma current can be softly terminated with a finite residual plasma density.

1. INTRODUCTION

An alternating current (AC) quasi-steady-state operation is an attractive alternative to pure steady state operation in D–T [1–3] and D–^{3}He tokamak [4] fusion reactors including the Next Step Device [5], because inductive current drive is highly efficient, reliable and technically simple. The inductive operation is practically independent of the plasma density and the species of the fusion products, in contrast to RF non-inductive current drive. These advantages will be more pronounced in a D–^{3}He tokamak reactor with a higher density ($\sim 4 \times 10^{20}$ m^{-3}) and a higher plasma current ($\sim$ 50 MA) than in a D–T tokamak reactor [4].

An experiment on AC operation was first demonstrated in the small STOR-1M tokamak ($R = 22$ cm, $a = 3.5$ cm) [6, 7], where the plasma current of +4 kA is ramped down and then up to −4 kA in the opposite direction. As the plasma was not completely lost during the current reversal phase, the second current rampup did not require a large loop voltage. Smooth current reversal was observed with considerable saving in the volt·second consumption. AC tokamak operation with reactor relevant current (±2 MA) has subsequently been demonstrated in JET [8, 9]. However, in the JET experiments, there was a 30 ms dwell time and the initiation of the second half-cycle required a large breakdown voltage. In an AC tokamak operation, the dwell time should be minimized (or eliminated) to reduce, for example, the time variation in the output temperature of the coolant in the blanket and the thermal load on the divertor. It is of interest to see whether the continuous current reversal without discharge dwelling, as observed in STOR-1M, can be achieved in a larger tokamak.

AC operation can be performed in a conventional tokamak if the circuits are modified properly for those of an ohmic heating primary, a vertical magnetic field and a position control system. In a small machine (such as STOR-1M) powered by non-electrolytic capacitors, the natural ringing LCR circuit can be exploited for AC operation because the cable resistance is relatively small owing to the short distance between the power supply and the poloidal coils on the tokamak. In a large machine (such as JET) controlled by the thyrister bridges, it is relatively easy to convert the single pulse ohmic circuit to AC. However, in the STOR-M tokamak ($R = 46$ cm, $a = 12$ cm) powered by an electrolytic capacitor, it is somewhat difficult to perform an AC operation because voltage reversible electrolytic capacitors are not usually available. In STOR-M, the LCR

Permanent addresses:
[a] Department of Electrical Engineering, Kyushu Tokai University, Toroku, Kumamoto, Japan.
[b] Advanced Laser and Fusion Technology, Inc., Station "T", Ottawa, Ontario, Canada.
[c] JET Joint Undertaking, Abingdon, Oxfordshire, UK.
[d] Australian National University, Canberra, Australia.

* Emeritus Professor, University of Saskatchewan, Canada.

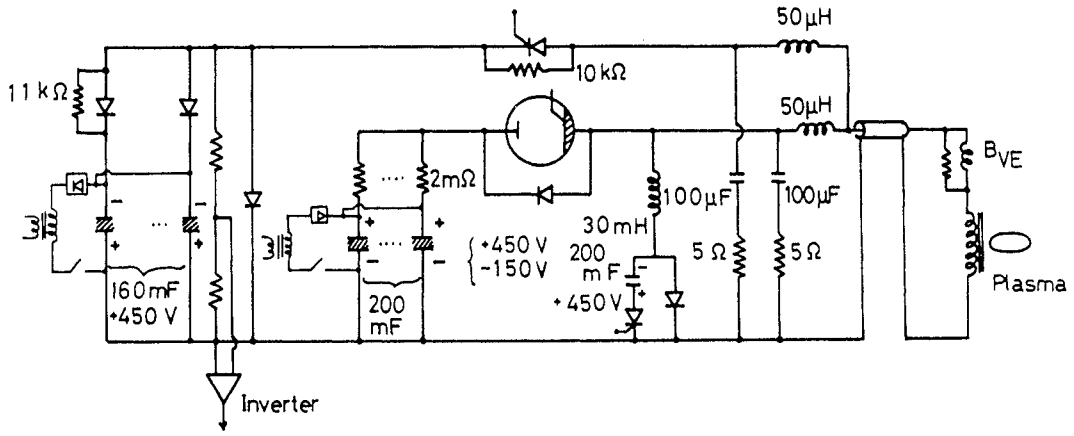

FIG. 1. Circuit diagram of the ohmic primary and vertical field coil systems for one cycle AC operation in the STOR-M tokamak.

circuit including the iron core transformer is characterized by a damped oscillating waveform due to the relatively large circuit resistance in the transmission line between the capacitor banks and the ohmic primary winding. To perform AC operation in STOR-M, a new primary circuit with voltage-reversible electrolytic capacitors has been designed and fabricated.

In this study, we demonstrate the AC operations with and without dwell time in the STOR-M tokamak with good reproducibility using a newly developed ohmic heating circuit. We describe the technological problems that have been overcome for AC operation in STOR-M and present the experimental data. The plasma current of +24 kA can be smoothly ramped down in 10 ms without disruptions (with a ramp-down rate of around 2.0 kA/ms) and then ramped up to between –20 and –24 kA without dwelling. The plasma density of up to $\sim 3.7 \times 10^{18}$ m^{-3}, which corresponds to a Murakami parameter of $\bar{n}R/B_t \sim 3.2(\pm 0.20) \times 10^{18}$ m$^{-2} \cdot$ T^{-1}, remains at the current reversal. Thus, we have found that AC operation without dwell time is possible at least up to the size of STOR-M when the plasma current is terminated softly with the residual plasma [10] and the initial loop voltage is a minimum when the dwell time is zero.

In Section 2, we briefly describe the experimental set-up. In Section 3, experimental results on AC operation with and without dwell time will be presented. The evolution of the plasma current and density is also displayed in the Murakami–Hugill diagram. In Section 4, discussions and a summary are given.

2. EXPERIMENTAL SET-UP

Experiments on AC plasma operation have been performed in the STOR-M tokamak with a major radius of $R = 46$ cm, a minor radius of $a = 12$ cm, a peak toroidal field of $B_t = 0.7$ T and peak plasma current $I_p \sim 30$ kA [11]. In these experiments, we constructed two sets of the electrolytic capacitor banks with a positive and negative charge to drive AC plasma currents. The first capacitor bank of 200 mF (+450 to −150 V) is for the positive plasma current and the second one of 160 mF (+450 to 0 V) is for the negative plasma current, as shown in Fig. 1. The first capacitor bank is composed of custom made voltage-reversible electrolytic capacitors, supplied by the Nichicon Corporation in Japan, and the second bank is composed of non-reversible electrolytic capacitors, which are protected by parallel diodes. The two banks are decoupled by a 50 μH inductor, which has negligible effects on the current waveform. After the voltage-reversible first bank was fired for the plasma current in the positive direction and the plasma current was reduced to zero, then the second negative capacitor bank with opposite polarity was triggered to produce AC operation. Therefore, flexible AC operations were possible by changing the dwell time from 0 to ~5 ms for studying the effect of the dwell time on the second initial loop voltage.

In the circuit shown in Fig. 1, the first and second capacitor banks are mutually coupled and do not work independently. Therefore, it is important to perform the circuit simulation to understand the whole discharge behaviour of the AC operation. The plasma

was simulated by copper wires ($\sim$0.2 mΩ) placed on the tokamak. The ratio of the first and second current peaks in this simulation experiment is 0.94 for the identical charging voltages of 160 V to the first and second capacitor banks. The second current peak is slightly larger, even with the smaller second bank capacitance, because the first bank has a protective resistance in series with the capacitor and the second bank has protective diodes and no such resistance. As the negatively charged first bank after the first plasma discharge is combined in parallel with the negatively charged second bank, the duration time of the second plasma current becomes longer than the first one by about 1.25 times. If the plasma resistance behaviour in the first and second discharges is identical in actual AC experiments, similar results on the plasma current can be obtained.

The feedback system for controlling the horizontal plasma position in the conventional unidirectional current operation was used in STOR-M AC experiments without any modification. However, an inverter for the plasma current signal was added to the position measuring system to operate the feedback system for either polarity of discharge current. This simple feedback system works only during the first positive plasma current and the current reversal phase. In fact, as will be seen, the second plasma is disruptively terminated after the current peak. A detailed explanation of the working principle of this scheme is given in Appendix A.

The line averaged electron density along the vertical chord of length $2a$ through the plasma centre has been measured by a 4 mm microwave interferometer with one quarter fringe corresponding to [10]

$$[\Delta\bar{n}]_{\mathrm{res}} = (\lambda/a)n_{\mathrm{c}}/4 = 0.58 \times 10^{18}\ \mathrm{m}^{-3}$$

which is the resolution limit in this electron density measurement. When the plasma radius changes, the line integrated density $2a[\Delta\bar{n}]_{\mathrm{res}} = 0.1392 \times 10^{18}\ \mathrm{m}^{-2}$ has to be used. As we assume no change in the plasma radius due to plasma shrinkage and plasma movement during the current reversal phase, the density step $[\Delta\bar{n}]_{\mathrm{res}}$ used here is a minimum. A visible spectrometer and a 17 GHz microwave reflectometer viewing horizontally are also used. Since the cut-off density for 17 GHz (O mode) is $n_{\mathrm{c}} \sim 3.6 \times 10^{18}\ \mathrm{m}^{-3}$, a reflectometer using the phase shift works as an interferometer below the cut-off density, employing the inner vacuum chamber as a reflecting mirror. The reflectometer was originally installed for measuring density fluctuations in the reflecting layer in the plasma.

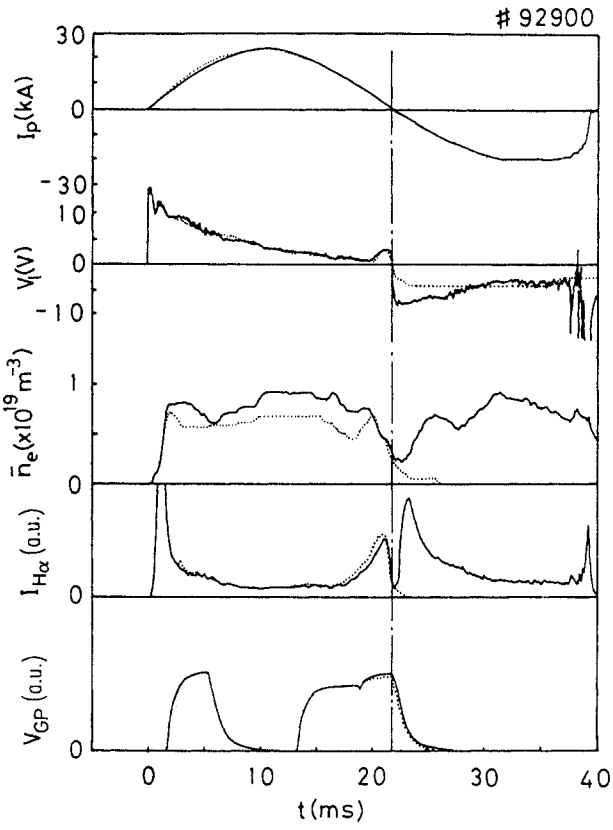

FIG. 2. Temporal evolution of one cycle AC discharge in the STOR-M tokamak (shot number 92 900): I_p is the plasma current, V_ℓ is the loop voltage, $\bar{n}_e$ is the line averaged electron density (0.58×10^{18} m^{-3}/step), I_{H_α} is the H_α emission intensity and V_{GP} is the pulse for gas puffing. The vertical dash-dot line indicates the current reversal time. The traces of a single pulse discharge with soft landing (shot number 92 971, see Fig. 6) shown by the dotted line are overlaid for direct comparison with AC operation.

3. EXPERIMENTAL RESULTS

3.1. AC operation

A typical temporal evolution of an AC discharge (shot number 92 900) is shown in Figs 2 and 3. The plasma current I_{p} decreases smoothly from the peak value of +24 kA to zero, and then increases to −20 kA in the negative direction with a rampdown rate of $\sim$ 2 kA/ms. The charging voltages for both capacitor banks were 160 V in this experiment. The loop voltage V_ℓ is about 4 V at the plasma current peak and no sharp voltage spikes have been observed during the current reversal phase. The plasma resistance of $R_{\mathrm{p}} \sim 0.20$ mΩ in the second negative current phase is larger than that of $\sim$ 0.167 mΩ in the first

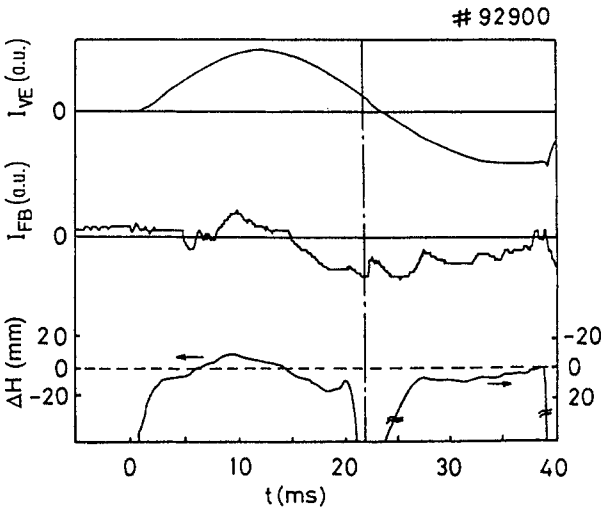

FIG. 3. Temporal evolution of one cycle AC discharge in the STOR-M tokamak (shot number 92 900): I_{VE} is the vertical equilibrium coil current, I_{FB} is the feedback coil current and ΔH is the plasma displacement. The vertical dash-dot line indicates the current reversal time.

positive current phase. The second plasma current finally disrupts because of the lack of the optimization of the feedback control system as explained previously and in Appendix A. We have also noticed that the second initial loop voltage is lower than the first one. The line averaged density $\bar{n}_e$ decreases from a steady value of 9.0×10^{18} m^{-3} to 3.7×10^{18} m^{-3} at the current reversal, and is further reduced to 2.0×10^{18} m^{-3} at 2.5 ms after the current reversal time indicated by the vertical dash-dot line and increases again in the second negative plasma current phase. The plasma density has been controlled by the gas puffing pulse V_{GP} using two PV-10 piezoelectric valves. The second and third gas puffing pulses before the current reversal were carefully adjusted by monitoring the electron density to achieve the direct transition to the subsequent plasma as well as in soft landing experiments [10]. The H_α line emission intensity I_{H_α} is maintained at a flat value in the plasma current regime larger than ~5 kA and increases just before the current reversal due to gas puffing. It then drops quickly, but remains finite at the current reversal, and increases again in the second plasma current phase.

Figure 3 shows the vertical equilibrium coil current I_{VE}, the feedback control current I_{FB} and the plasma position signal ΔH. In STOR-M AC experiments with a combined circuit consisting of an ohmic primary and a vertical equilibrium current, the feedback control current plays an important role in providing a total equilibrium vertical field proportional to the plasma current during the current reversal phase, as explained in Appendix B. In order to match the total vertical field to the plasma current in the startup phase of the second negative plasma current, the feedback control current was externally modified by a voltage pulse as shown in Fig. 3. This technique enhances the reproducibility of AC operation. In the previous soft landing experiments [10] it has been observed that inward movement of plasma before the current termination was important for smooth current termination. Therefore, adjusting the plasma position before the current reversal by the voltage pulse on the feedback control current was also effective in ensuring a smooth transition.

A Hugill diagram is plotted in Fig. 4 together with the time variations of the density and of the plasma current during the current rampdown phase with $|I_p| < 15$ kA. The relation $1/q_a = (\mu_0 R/2\pi a^2 B_t) I_p$ has been used for this calculation and the plasma current profile was assumed to have no reverse current layer for simplifying the analyses. This assumption may be justified if gas puffing could suppress the negative current layer. The plasma density (or $\bar{n}R/B_t$) decreases with the decrease in the plasma current, and then reaches a finite offset value of $\bar{n}R/B_t \sim (3.2 \pm 0.2) \times 10^{18}$ m$^{-2} \cdot$ T^{-1} at $1/q_a = 0$. We should note that the change in the toroidal field is taken into account for this analysis because the toroidal field is maximum at the plasma breakdown phase and decreases monotonically. In the negative current phase ($1/q_a < 0$), the density decreases further to $\sim (2.0 \pm 0.2) \times 10^{18}$ m$^{-2} \cdot$ T^{-1}, and then increases. It is interesting to note that the operating point of the density in the Hugill diagram follows the straight lines of $1/q_a \sim +0.01 \bar{n}R/B_t (10^{-18}$ m$^2 \cdot$ T) just before the current reversal as indicated by the dash-dot line, corresponding to the density 'shoulder' indicated in Fig. 4, as observed in the soft landing experiments [10]. The density 'shoulder' just before the current reversal is needed to make the direct transition to the next discharge. We also notice that the operating point follows a steeper straight line: $1/q_a \sim +0.02 nR/B_t (10^{-18}$ m$^2 \cdot$ T) during the startup phase in the second plasma current. This may be due to the symmetric change (the decrease and increase) in the ohmic heating power during the current reversal phase. For comparison, the density and Murakami parameter at the zero plasma current observed during AC operation in the STOR-1M tokamak ($R = 22$ cm, $a = 3.5$ cm, $B_t = 1$ T) are $\bar{n} \sim (3 \pm 1) \times 10^{18}$ m^{-3} and $\bar{n}R/B_t \sim (0.66 \pm 0.22) \times 10^{18}$ m$^{-2} \cdot$ T^{-1} at $1/q_a = 0$

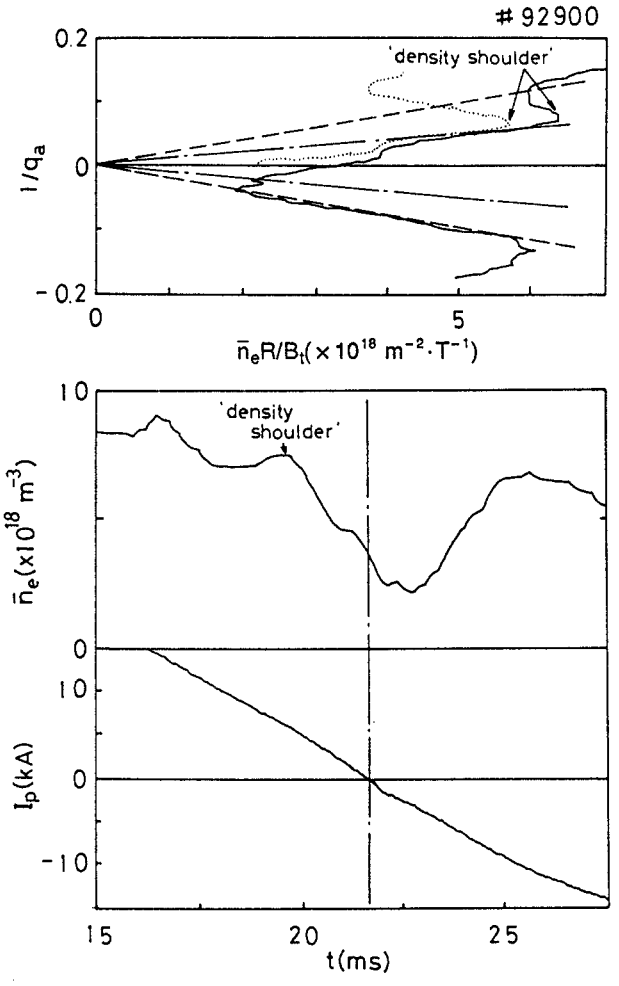

FIG. 4. Density behaviours during the current reversal phase with $|I_p| < 15$ kA in the Murakami–Hugill diagram corresponding to Fig. 2. Expanded traces of the density and plasma current are shown at the bottom. The dotted line shows the trace of a single pulse discharge with a soft landing (shot number 92 971).

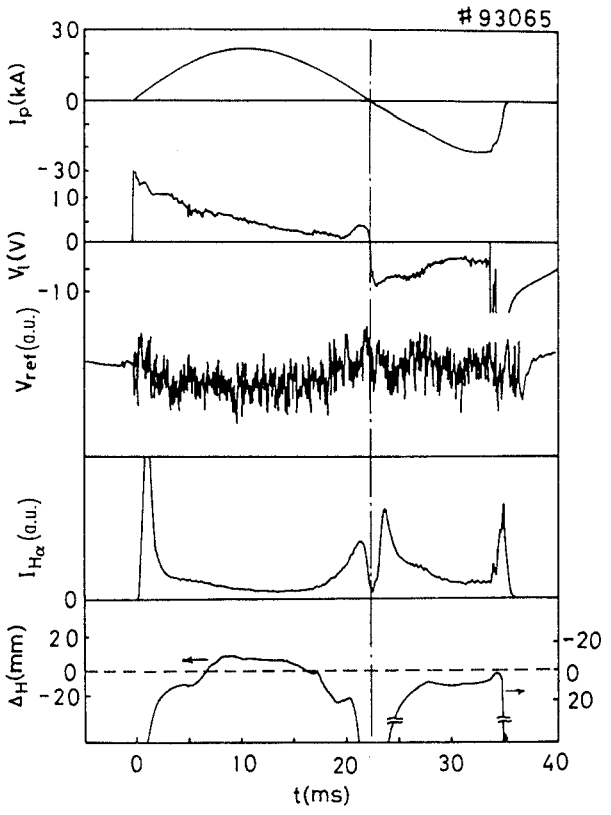

FIG. 5. Microwave reflectometer signal (V_{refl}) during the current reversal in a one cycle AC discharge (shot number 93 065).

with and without gas puffing [6, 7]. It is still unknown what determines these parameters.

A signal of a 17 GHz microwave reflectometer viewing the plasma horizontally through a window in the outer part of the tokamak is shown in Fig. 5 for AC operation. Unfortunately, the line averaged density was not obtained in this shot because of a failure of the microwave tube. Therefore, the quantitative characteristics of, for example, the reflecting layer are uncertain in this case. However, the reflectometer phase signal during the current reversal indicates the presence of the plasma with a density $\bar{n}_c \sim 3.6 \times 10^{18}$ m^{-3} [10].

3.2. Comparison with a single pulse with soft landing

In order to check the finite density at the current reversal in AC operation, we have compared AC operation with single pulse operation by switching off the second capacitor bank. In Fig. 6, the temporal evolution of a single pulse discharge with a soft landing (shot number 92 971) is shown. (In Fig. 2, the same result is also overlaid with the dotted lines for direct comparison.) It can be clearly seen that the plasma density remains for about 4 ms after the current termination. Thus, we can confirm that the signal from the density measurement returns to zero level after the current termination, as observed in the previous soft landing experiments [10]. The plasma current waveform, loop voltage, density and H_α in this single pulse operation behave similarly to the first half-cycle of the AC operation in Fig. 2. The time variation of the density and plasma current for the single pulse discharge is plotted on the Hugill diagram in Fig. 4 together with AC operation.

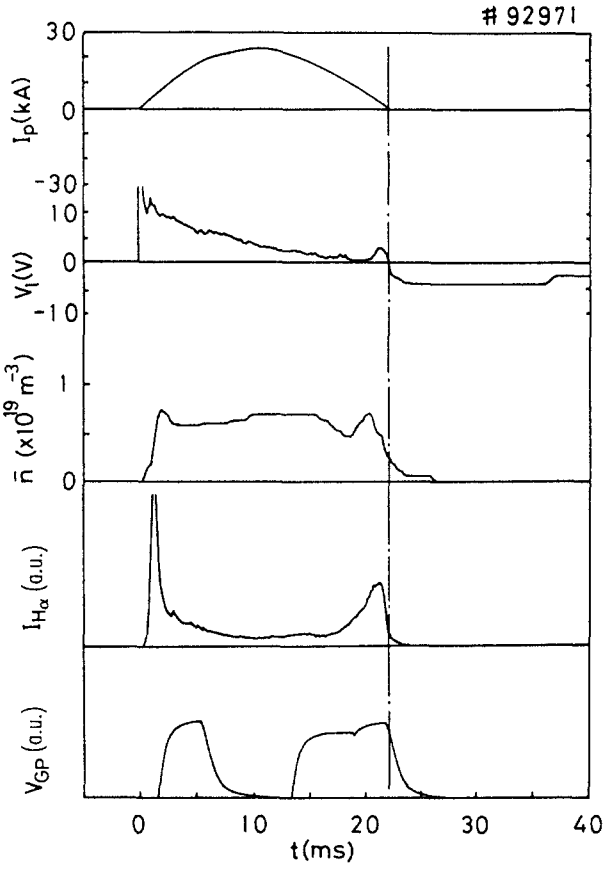

FIG. 6. Temporal evolution of a single pulse discharge in the STOR-M tokamak (shot number 92 971) for comparison with AC operation.

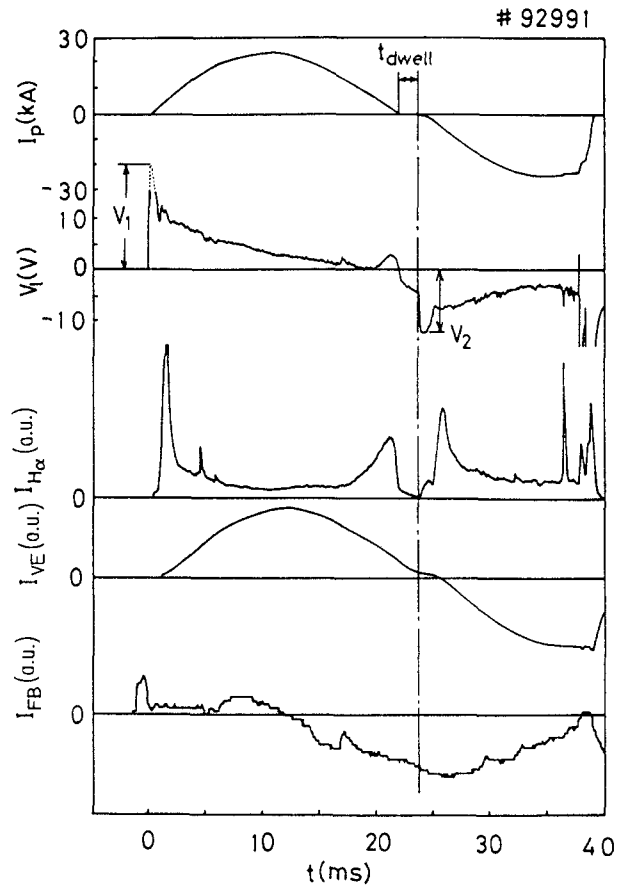

FIG. 7. Temporal evolution of one cycle AC discharge with a finite dwell time in the STOR-M tokamak (shot number 92 991): I_p is the plasma current, V_l is the loop voltage and I_{H_α} is the H_α emission intensity.

3.3. The effect of dwell time on AC operation

Benefitting from the two separate capacitor banks, the dwell time can be changed as done in JET [9] by delayed triggering of the second negative bank. The temporal evolution of the AC operation with a dwell time of ~ 2.5 ms (shot number 92 991) is shown in Fig. 7. The first positive pulse has a smooth current rampdown and the second plasma evolves after the dwell time. It is seen that the maximum loop voltage for the second negative current is about 12.1 V, which is larger than that without a dwell time. This type of discharge is also very reproducible.

We have surveyed the dependence of the second initial loop voltage on the dwell time. The definitions of the loop voltage and of the dwell time are described in Fig. 7. As shown in Fig. 8, the loop voltage is a minimum, around 8.0 V, at zero dwell time, and increases with the dwell time. For dwell times longer than 4 ms, the second initial loop voltage is exactly the same as that in the first positive pulse. We see that the remaining density does not affect the second discharge for dwell times longer than 4 ms. Since a density remains for about 4 ms after current termination in the single pulse operation, as shown in Fig. 6, we now see that the time the density lasts after current termination is comparable to a dwell time of 4 ms, as found in Fig. 8. Although we had intended to plot the relationship between the remaining density and the dwell time, the line averaged density was, unfortunately, not obtained in the experiment on the dwell time effect owing to a failure of the microwave tube.

We have tried to apply the second negative pulse at 1.3 ms earlier than the current reversal time ('negative dwell time'). The result is shown in Fig. 9. The plasma current decreases rapidly by application of the negative voltage before the current reversal, and then slowly increases to the negative direction. Therefore, the loop voltage has a small spike at the current startup phase. In Fig. 8, this voltage has been plotted at a negative dwell time of -1.3 ms. Contrary

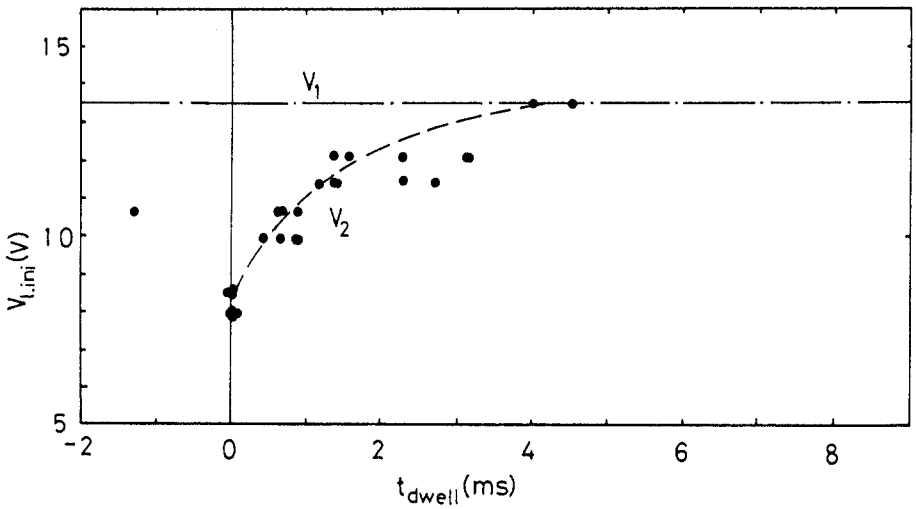

FIG. 8. Initial loop voltage (V_2) for the second negative current plotted against the dwell time (t_{dwell}). Definitions of V_2 and t_{dwell} are also shown in Fig. 7.

to expectations, it was somewhat difficult to produce the second negative plasma current reproducibly, and the second initial loop voltage was increased again with respect to the 'negative dwell time'. This may be due to unoptimization of the total vertical field in the startup phase of the second plasma current.

4. DISCUSSION AND SUMMARY

In this experiment on STOR-M, modification of the position feedback controller is not complete, and the plasma position is not well controlled in the negative plasma current phase. Therefore, the plasma current has a disruption at the end of the second negative plasma current phase in all the shots. This can be confirmed from the fact that the plasma resistance in Fig. 2 is lower at the plasma current peak in the first positive phase than that in the second negative plasma current phase. Since the charging voltage for both capacitor banks is the same in this experiment, identical plasma currents should be obtained for the same plasma resistance. Therefore, the first plasma may have a higher plasma temperature than that in the second plasma, or the impurity content in the first plasma may be lower than that in the second plasma. This is also inferred from the difference of the H_α intensity signals, which is almost twice as large in the second discharge, as shown in Fig. 2. Therefore, the second plasma has a stronger plasma–wall interaction than the first plasma due to incomplete optimization of the feedback control system.

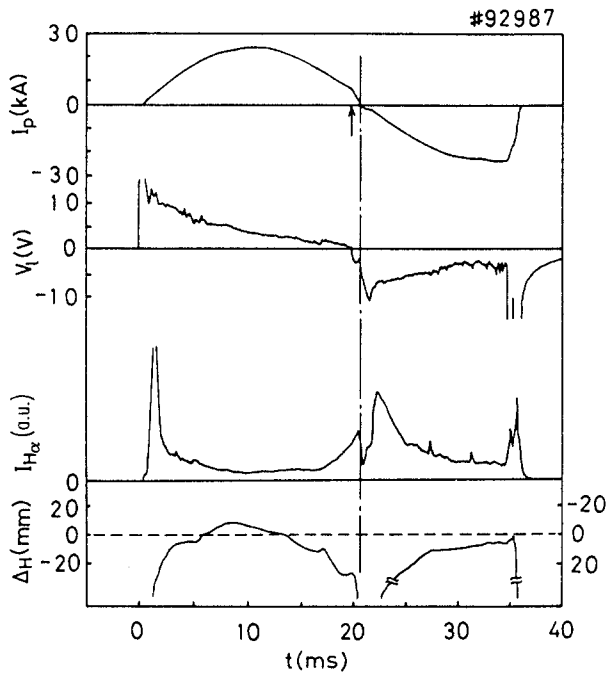

FIG. 9. Temporal evolution of a one cycle AC discharge with triggering of the second capacitor bank prior to termination of the first positive plasma current. ΔH is the plasma displacement.

In summary, we have demonstrated one cycle AC plasma operation without a dwell time in the STOR-M tokamak with a good reproducibility. A plasma current of +24 kA can be smoothly ramped down in 10 ms with a rampdown rate of around

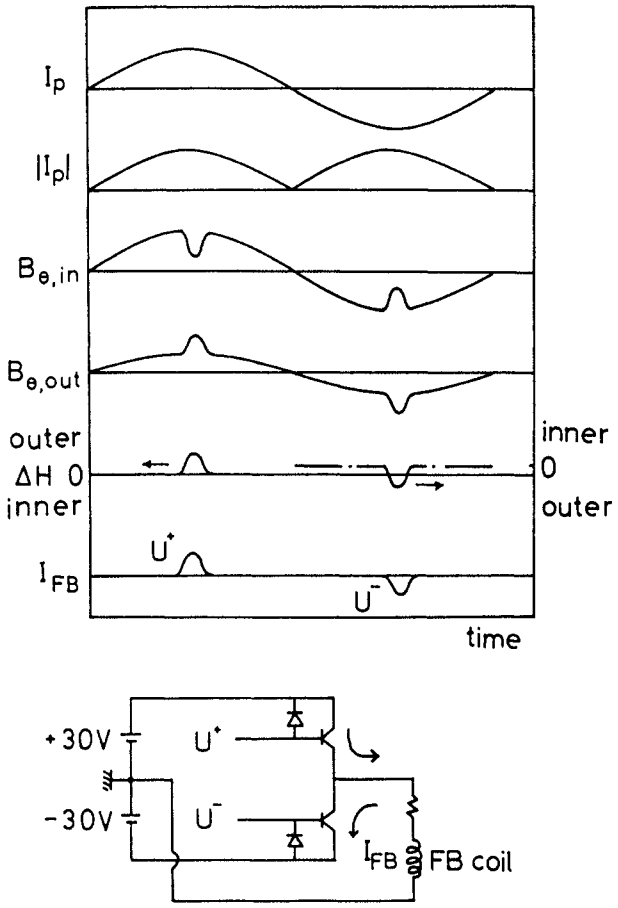

FIG. 10. Schematic waveforms to explain how the feedback control system works for AC operation in STOR-M and a schematic diagram of the feedback control circuit.

2.0 kA/ms and then ramped up to between −20 and −24 kA without a dwell time. A plasma density of up to 3.7×10^{18} m^{-3} remains at the current reversal, as is also observed in the soft landing experiments. The key to successful, reproducible and direct transitions in AC tokamak operations on STOR-M is to control both the total vertical field by the feedback control system and the plasma density by careful gas puffing during the current reversal phase. This experiment has also specifically demonstrated that the initial loop voltage for the second negative current is minimized when the dwell time approaches zero, and AC operation without a dwell time is possible whenever the plasma current can be softly terminated with a finite residual plasma density. Smooth termination of the second plasma current is necessary for 1.5 cycle AC operation, which further requires the modification of the AC feedback control system.

Appendix A

WORKING PRINCIPLE OF THE FEEDBACK SYSTEM FOR AC OPERATION

The working principle of the feedback system is explained as follows. The horizontal plasma displacement ΔH given [12] by

$$\Delta H = \frac{a^2}{4R}\left[\left(\frac{r_m^2}{a^2} - 1\right) - 2\ln\left(\frac{a}{r_m}\right)\right] + \frac{\pi r_m^2}{2\mu_0 |I_p|}\left[(B_{\theta,out} - B_{\theta,in})\left(1 - \frac{a^2}{r_m^2}\right) - (B_{\rho,up} - B_{\rho,down})\left(1 + \frac{a^2}{r_m^2}\right)\right] \quad (1)$$

where $r_m = 17$ cm is the radius of the probe position from the plasma centre, and $B_{\theta,out}$ and $B_{\theta,in}$ are the poloidal components of the magnetic field measured by magnetic probes placed at the outboard plane and at the inboard plane, respectively. $B_{\rho,up}$ and $B_{\rho,down}$ are the radial components of the magnetic field measured by magnetic probes placed at the upper position and at the lower position, respectively, and $|I_p|$ is the absolute value of the plasma current provided by the inverter. As the magnetic fields $B_{\theta,out} - B_{\theta,in}$ and $B_{\rho,up} - B_{\rho,down}$ change sign in the second negative plasma current phase and the plasma current remains positive due to the inverter, the plasma position (inward or outward) was inverted in the second negative plasma current phase. As schematically shown in Fig. 10, when the plasma moves outward in the first positive plasma current phase, ΔH has a positive signal, and a positive feedback signal voltage U^+ must be applied to increase the current in the vertical coil to push the plasma inward [13]. On the other hand, when the plasma moves outward in the second negative plasma current phase, ΔH has a negative signal, as seen from Eq. (1), and thus a negative feedback signal voltage U^- must be applied to increase the vertical coil current in the negative direction because the vertical field direction is now negative. Thus, the feedback system works in some range as in the conventional unidirectional discharge. The first term in Eq. (1) yields 13.3 mm for STOR-M, which provides the offset for AC operation. As the feedback system is optimized for normal operation and first plasma current, the second negative plasma current phase needs additional optimization. In fact, the second plasma is disruptively terminated after the current peak, as shown in Fig. 2.

The first method of overcoming this problem is to apply a positive bias voltage on the plasma position signal ΔH for optimizing the plasma position during the second negative plasma current phase. At present, the plasma is interpreted to be at the outward position by the position measurement system during the second plasma current phase, and thus a large feedback control current is applied. Therefore, the plasma in a real situation may be at the inward position. The second method is to invert the magnetic field signals from the plasma position sensors, and the polarities of the transistor control signals U^+ and U^- shown in Fig. 10 would be switched during the negative plasma current phase. The optimization of the feedback control with these modifications will be conducted in the near future prior to attempting to achieve a 1.5 cycle AC operation.

Appendix B

ROLE OF THE FEEDBACK CONTROL CURRENT IN A COMBINED CIRCUIT FOR AC OPERATION

As shown in Figs 2 and 3, the primary current I_{oh} proportional to I_{VE} is larger than the plasma current I_p at the current reversal phase owing to the magnetizing current for inducing the plasma current by the ohmic primary current. As the vertical equilibrium coil current is proportional to the ohmic primary current in this combined circuit system, the resultant offset from the optimum vertical field has to be supplied by a feedback coil. During the current reversal phase, the feedback current I_{FB} is increased in the negative direction, according to the plasma inward movement signal, and reaches a negative saturation value determined by the feedback circuit itself. As it is difficult to control the feedback current by the plasma parameter optimization during the current reversal phase, a rectangular voltage pulse of 12.0 V with 1.5 ms duration was externally applied to the feedback control signal. Matching the total vertical field to the plasma current is now possible in the startup phase of the second negative plasma current. As shown in Fig. 3, the I_{FB} signal has a hump after the current reversal phase due to this external pulse. Careful control of the feedback current during the current reversal is, therefore, an important technological factor in achieving smooth AC operation in the combined circuit.

ACKNOWLEDGEMENTS

We gratefully thank Y. Yaguchi of Nichicon Corporation in Japan for technical information on voltage-reversible electrolytic capacitors. The technical assistance provided by J. Ratzlaff is gratefully acknowledged. One of the authors (O.M.) gratefully acknowledges encouragement given by the faculty members of the Department of Electrical Engineering at Kyushu Tokai University.

This research was sponsored by the Natural Sciences and Engineering Research Council of Canada. The travel of O. Mitarai was supported by the Japan Society for the Promotion of Science and by NSERC, Canada.

REFERENCES

[1] MITARAI, O., et al., AC tokamak reactor, in Plasma Science (Proc. IEEE Int. Conf. Saskatoon, 1986), IEEE, New York (1986) 39.
[2] MITARAI, O., et al., Fusion Technol. **15** (1989) 204.
[3] MITARAI, O., et al., Fusion Technol. **20** (1991) 285.
[4] MITARAI, O., Fusion Eng. Des. **26** (1995) 605.
[5] REBUT, P.H., A Fusion Reactor: Continuous or Semi-continuous?, Rep. JET-P(92)65, JET Joint Undertaking, Abingdon (1992).
[6] MITARAI, O., et al., Bull. Am. Phys. Soc. **29** (1984) 1337; Nucl. Fusion **27** (1987) 604.
[7] MITARAI, O., et al., Nucl. Fusion **32** (1992) 1801.
[8] HUART, M., et al., in Fusion Engineering (Proc. 14th Symp. San Diego, 1991), Vol. 1, IEEE, New York (1992) 181.
[9] TUBBING, B.J.D., et al., Nucl. Fusion **32** (1992) 967.
[10] MITARAI, O., et al., Plasma Phys. Control. Fusion **35** (1993) 711.
[11] ZHANG, W., et al., Phys. Fluids B **4** (1992) 3277.
[12] NINOMIYA, H., SUZUKI, N., Jpn. J. Appl. Phys. **21** (1982) 1323.
[13] EMAAMI, M., Modeling and Control of Plasma Position in the STOR-M Tokamak, Rep. PPL-112, Univ. of Saskatchewan, Saskatoon (1990).

(Manuscript received 12 September 1995
Final manuscript accepted 3 April 1996)